Biol. Chem., Vol. 393, pp. 391–401, May 2012 • Copyright © by Walter de Gruyter • Berlin • Boston. DOI 10.1515/hsz-2011-0264

Stromal cell-associated expression of kallikrein-related peptidase 6 (KLK6) indicates poor prognosis of ovarian cancer patients

Lina Seiz[1], Julia Dorn[1], Matthias Kotzsch[2], Axel Walch[3], Nicolai I. Grebenchtchikov[4], Apostolos Gkazepis[1], Barbara Schmalfeldt[1], Marion Kiechle[1], Jane Bayani[5], Eleftherios P. Diamandis[5], Rupert Langer[6], Fred C.G.J. Sweep[4], Manfred Schmitt[1] and Viktor Magdolen[1,*]

[1] Klinische Forschergruppe der Frauenklinik der Technischen Universität München, Klinikum rechts der Isar, Ismaninger Str. 22, D-81675 Munich, Germany
[2] Institut für Pathologie, Technische Universität Dresden, Dresden, Germany
[3] Institut für Pathologie, Helmholtz Zentrum München, Neuherberg, Germany
[4] Department of Laboratory Medicine, Radboud University Nijmegen Medical Centre, Nijmegen, The Netherlands
[5] Department of Pathology and Laboratory Medicine, Mount Sinai Hospital, Toronto, Canada
[6] Institut für Pathologie, Technische Universität München, Munich, Germany

* Corresponding author
e-mail: viktor.magdolen@lrz.tum.de

Abstract

Several members of the human kallikrein-related peptidase family, including KLK6, are up-regulated in ovarian cancer. High KLK6 mRNA or protein expression, measured by quantitative polymerase chain reaction and enzyme-linked immunoassay, respectively, was previously found to be associated with a shortened overall and progression-free survival (OS and PFS, respectively). In the present study, we aimed at analyzing KLK6 protein expression in ovarian cancer tissue by immunohistochemistry. Using a newly developed monospecific polyclonal antibody, KLK6 immunoexpression was initially evaluated in normal tissues. We observed strong staining in the brain and moderate staining in the kidney, liver, and ovary, whereas the pancreas and the skeletal muscle were unreactive, which is in line with previously published results. Next, both tumor cell- and stromal cell-associated KLK6 immunoexpression were analyzed in tumor tissue specimens of 118 ovarian cancer patients. In multivariate Cox regression analysis, only stromal cell-associated expression, besides the established clinical parameters FIGO stage and residual tumor mass, was found to be statistically significant for OS and PFS [high vs. low KLK6 expression; hazard ratio (HR), 1.92; p=0.017; HR, 1.80; p=0.042, respectively]. These results indicate that KLK6 expressed by stromal cells may considerably contribute to the aggressiveness of ovarian cancer.

Keywords: cancer biomarker; immunohistochemistry; kallikrein-related peptidase 6; KLK6; ovarian cancer; prognosis.

Introduction

The family of human tissue kallikrein-related peptidases (KLKs) constitutes a group of 15 secreted serine proteases, which are coexpressed in diverse normal and malignant human tissues. Clustered together on the chromosomal locus 19q13.3-4, the *KLK* genes share remarkable homology at both nucleotide and protein levels (Diamandis et al., 2000; Debela et al., 2008; Goettig et al., 2010). Although *KLK* gene expression underlies the regulation by steroid hormones and DNA methylation (Yousef and Diamandis, 2001; Christophi et al., 2004; Pampalakis and Sotiropoulou, 2007; Lundwall and Brattsand, 2008; Bayani and Diamandis, 2011), the enzymatic activity of several KLKs is considered to be further modulated by physiological inhibitors or allosterically in the presence of zinc (Borgoño and Diamandis, 2004; Debela et al., 2006a,b; Luo and Jiang, 2006). In previous studies, aberrant expression profiles of KLK proteases, including KLK6, have been linked to neurodegenerative diseases and skin disorders as well as to malignant conditions, such as ovarian, breast, and prostate cancer or malignant melanoma (Sidiropoulos et al., 2005; Pampalakis et al., 2006; Krenzer et al., 2011). Unsurprisingly, kallikrein-related peptidases came in the focus as potential diagnostic, prognostic, and/or predictive tumor markers not only in hormone-regulated malignancies but also in several other cancers, including brain, head and neck, gastrointestinal, renal, and lung neoplasms (Emami and Diamandis, 2008; White et al., 2010).

KLK6, formerly known as zyme, protease M, or neurosin, is abundantly expressed in the central nervous system (CNS) but not or only weakly in the normal ovary (Yousef and Diamandis, 2001; Petraki et al., 2006; Shaw and Diamandis, 2007). The regulation of KLK6 activity is mediated mainly through (auto-)proteolytic activation or inactivation, whereas the most efficient inhibition is achieved by endogenous antithrombin III (Magklara et al., 2003; Bayés et al., 2004). KLK6 displays trypsin-like specificity and, together with many other proteases, participates in highly organized proteolytic cascades (Debela et al., 2006b; Yoon et al., 2007, 2008; Beaufort et al., 2010), which have been suggested to play

crucial roles in diverse (patho-)physiological processes, including semen liquefaction, skin desquamation, neurodegeneration, and cancer (Sotiropoulou et al., 2009).

High abundance of KLK6 in CNS prompted further investigation of its functional role in the field of neurological disorders. Indeed, several studies suggest an involvement of KLK6 in the pathogenesis of Alzheimer and Parkinson disease because KLK6 has been shown to degrade both amyloid precursor protein and α-synuclein (Iwata et al., 2003; Yousef et al., 2003; Ashby et al., 2010). In patients with multiple sclerosis, elevated KLK6 serum levels are thought to drive disease progression and thus aggravate neurological disability, due to neurotoxic properties causing neuron cell death and inhibition of axon outgrowth (Scarisbrick et al., 2008). Still, the potential of KLK6 as a serological marker for multiple sclerosis is currently a subject of discussion (Hebb et al., 2010).

Regarding ovarian cancer, there is a growing number of evidence suggesting that KLK6 is involved in tumor growth and progression and represents a useful biomarker for screening, diagnosis, prognosis, and prediction (Bayani and Diamandis, 2011). Overexpression of KLK6 in ovarian cancer cells, together with other KLKs, resulted in increased invasion in Matrigel invasion assays and tumor burden in a nude mouse model (Prezas et al., 2006). Determination of KLK6 and/or KLK13 in addition to carbohydrate antigen 125 (CA125 or MUC16), presently the best-established marker in clinical application for diagnosis and therapy monitoring of ovarian cancer, improves the sensitivity and specificity of CA125 as a diagnostic tool (Diamandis et al., 2003; White et al., 2009a). Otherwise, KLK6 and other KLKs were found to be up-regulated in CA125-negative ovarian cancer, implicating the possibility that KLKs could be useful biomarkers complementary to CA125 (Rosen et al., 2005). Moreover, a score based on clinical factors, together with KLK6 and KLK13, can be applied to predict efficiency of surgical treatment (Dorn et al., 2007).

Several research groups have retrospectively surveyed expression of KLK6 in relation to clinical and histomorphological factors. Elevated KLK6 protein or mRNA levels, quantitatively analyzed either by enzyme-linked immunoassay (ELISA) or quantitative polymerase chain reaction (PCR), were found to be associated with a more invasive cancer phenotype, late tumor (FIGO) stages, higher tumor grade, suboptimal debulking, as well as serous and undifferentiated histotypes (Shan et al., 2007; White et al., 2009b; Koh et al., 2011). Most importantly, up-regulated KLK6 expression was also identified as a strong indicator of shortened overall survival (OS) and higher risk of disease recurrence in ovarian cancer patients (Hoffman et al., 2002; Kountourakis et al., 2008; Oikonomopoulou et al., 2008; White et al., 2009b). Finally, KLK6 may also serve as a predictive marker because higher KLK6 serum levels are associated with chemoresistance (Diamandis et al., 2003; Oikonomopoulou et al., 2008).

Because KLK6 seems to play a crucial role in ovarian cancer, the aim of the present study was to assess its expression pattern in various normal and ovarian cancer tissues by immunohistochemistry and to evaluate the prognostic impact of both tumor cell- and stromal cell-associated KLK6 expression in ovarian cancer patients.

Results

Generation and characterization of monospecific polyclonal antibodies directed to KLK6

For immunization of rabbits, purified and refolded recombinant (non-glycosylated) human KLK6 (rec-KLK6), carrying an N-terminal extension of 17 amino acids encompassing a histidine $(His)_6$-tag and an enterokinase (EK) cleavage site (Asp-Asp-Asp-Asp-Lys) was used. Monospecific, polyclonal antibodies directed to KLK6 were purified from the blood of animal #623 (pAb 623A) by affinity chromatography against a peptide of KLK6 encompassing amino acids 109 to 119 (according to the chymotrypsin numbering; Goettig et al., 2010). Based on the X-ray structure of human KLK6 (Bernett et al., 2002; Gomis-Rüth et al., 2002), this region forms a surface-exposed flexible loop. Such loop structures are generally known to be immunogenic. Furthermore, the selected region is not highly conserved among the members of the KLK family, which minimizes the chance for cross-reaction of the monospecific polyclonal antibodies with other members of the KLK family. In fact, in a previous study, monospecific polyclonal antibodies directed against the corresponding region in KLK4 were found to be very specific and not to cross-react with other KLK proteases (Seiz et al., 2010).

The reaction pattern of affinity-purified pAb 623A was initially tested in a so-called one-side ELISA assay (Seiz et al., 2010), in which microtiter plates were coated with testing proteins and peptides, and then, the reaction of pAb 623A with these attached proteins/peptides was monitored. pAb 623A strongly reacted with its immunogen, rec-KLK6, and with the peptide $KLK6_{109–119}$ used for affinity purification. No reaction was observed, neither with peptides covering the $(His)_6$-tag and the EK cleavage site nor with irrelevant proteins, such as rec-KLK7, carrying the identical N-terminally located 17-amino acid extension as rec-KLK6 (data not shown). Furthermore, in Western blot analysis, pAb 623A was found to be highly specific for KLK6, as no cross-reaction with other KLK proteases was observed (Figure 1A). Human brain is known to express rather high amounts of KLK6 (Shaw and Diamandis, 2007). Therefore, we used protein extracts from human brain as the positive control, and extracts from skeletal muscle as the negative control (Shaw and Diamandis, 2007), for further characterization by Western blotting (Figure 1B). KLK6 has been reported to be N-glycosylated at Asn134 (Kuzmanov et al., 2009), and thus, the observed strong and rather broad signal in the brain around 43 kDa is as expected (non-glycosylated KLK6 displays an apparent molecular weight of ~31 kDa). In skeletal muscle extracts, no KLK6 reaction was detected using pAb 623A in the Western blot.

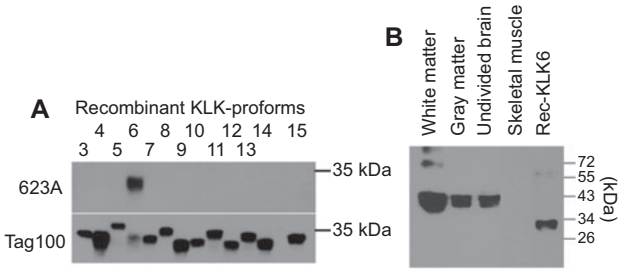

Figure 1 Analysis of specificity of monospecific pAb 623A by Western blot analysis.

(A) Recombinant pro-forms of KLK3–15 (~1 µg each) were subjected to 12% SDS-PAGE, blotted onto a PVDF membrane, and then incubated with pAb 623A. Only pro-KLK6 (with an apparent molecular weight of ~31 kDa), but not pro-KLK3–5 and pro-KLK7–15, reacted with pAb 623A. Thus, no cross-reactivity of pAb 623A with KLK3–5,7–15 was observed. The proper transfer of KLK proteins onto the membrane was verified by reaction with an antibody directed against the C-terminally located Tag100 epitope present in all recombinant pro-KLK proteins. (B) Glycosylated KLK6 was detected in tissue extracts from the central nervous system (~20 µg/lane) by pAb 623A. Compared with non-glycosylated rec-KLK6, a higher molecular mass for KLK6 was found in tissue extracts of the white matter mainly consisting of myelinated axon tracts, in tissue extracts of the gray matter containing neural cell bodies, and in undivided brain extracts. Skeletal muscle tissue extract (~20 µg) was used as a negative control.

Immunohistochemical analysis of KLK6 expression in healthy adult human tissues using pAb 623A

In immunohistochemical analyses of representative sections of healthy adult human tissues, pAb 623A was used to probe these tissues for detection of KLK6. In a variety of normal adult tissues, KLK6 expression was detected: strong KLK6 expression was observed in the brain (Figure 2A), whereas moderate immunostaining was found in the liver, kidney, ovary (Figure 2B–D), breast, lung, and skin (data not shown). In normal pancreas, skeletal muscle (Figure 2E and F), colon, and prostate (data not shown), KLK6 was not detected by reaction with pAb 623A. The observed KLK6 immunoexpression pattern in normal adult tissues is perfectly in line with previous results obtained by determination of KLK6 antigen levels in adult tissue extracts applying a highly specific KLK6 ELISA (Shaw and Diamandis, 2007).

Expression pattern of KLK6 in ovarian cancer tissue and its association with clinical and histomorphological parameters

To evaluate protein expression of KLK6 in ovarian cancer by immunohistochemistry and its impact on patients' prognosis, tumor tissue samples of 118 ovarian cancer patients, represented on seven tissue microarrays, were investigated using pAb 623A. In the majority of cases, distinct cytoplasmic KLK6 immunostaining was observed in malignant epithelial tumor cells and also, with lower frequency, in surrounding stromal cells. Based on classical morphological features, these cells most probably represent (myo-)fibroblasts and tissue macrophages (Figure 3).

For estimation of KLK6 immunoreactivity, a semiquantitative score, ranging from 0 (negative) to 12 (strongly positive), based on KLK6 staining intensity and percentage of KLK6-positive cancer cells (KLK6-Tc) and KLK6-positive stromal cells (KLK6-Sc), respectively, was used. We found a moderate but significant correlation between KLK6-Tc and KLK6-Sc immunoscore values using Spearman rank correlation analysis (r_s=0.53, p<0.001). A distinctly elevated KLK6 expression was observed in tumor cells vs. stromal cells in tumor tissue: the mean score value of KLK6-Tc (3.81) was much higher than that of KLK6-Sc (0.79). The frequency of scores greater than zero was much higher for tumor cells compared with stromal cells (KLK6-Tc >0, 90 cases vs. KLK6-Tc=0, 28 cases; KLK6-Sc >0, 24 cases vs. KLK6-Sc=0, 93 cases). For all statistical analyses, the median score values of both KLK6-Tc (median=4) and KLK6-Sc (median=0) were chosen to classify immunohistochemical KLK6 expression as high or low (KLK6-Tc low with immunoscore ≤4 as cutoff, 84 cases; KLK6-Tc high with immunoscore >4, 34 cases; KLK6-Sc low with immunoscore 0, 93 cases; KLK6-Sc high with immunoscore >0, 24 cases).

The relationship of KLK6 immunoscore values with relevant clinical and histomorphological parameters of ovarian cancer patients is summarized in Table 1. A significant association was observed between high KLK6-Sc score values and poorly differentiated tumors (nuclear grade G3 vs. G1/2) as well as the presence of affected lymph nodes (p=0.028 and p=0.020, respectively). Otherwise, there was no significant association of KLK6-Sc score values with other clinical/histomorphological parameters. Regarding KLK6-Tc score values, KLK6 immunoexpression did not differ significantly between tumors in relation to any of the clinical or histomorphological parameters.

Association of KLK6 expression and clinical/histomorphological parameters with patients' survival

The strength of association between clinical/histomorphological parameters and KLK6 immunoexpression with patients' outcome defined as progression-free survival (PFS) and OS is presented in Table 2. In univariate Cox regression analysis, all established clinical and histomorphological variables such as age, FIGO stage, nuclear grade, residual tumor mass, and ascitic fluid volume were predictors for OS in the ovarian cancer cohort. Likewise, in univariate analysis of PFS, all of the clinical and histomorphological parameters reached statistical significance (Table 2).

Moreover, in univariate Cox regression analysis, we found a significant association between high KLK6-Sc score values in tumor tissue and an increased risk of death [hazard ratio (HR), 1.80; 95% confidence interval (CI), 1.08–2.99; p=0.024] and a trend toward statistical significance for the correlation of high KLK6-Sc score values with tumor progression (HR, 1.68; 95% CI, 0.97–2.92; p=0.066). In case of KLK6-Tc, high

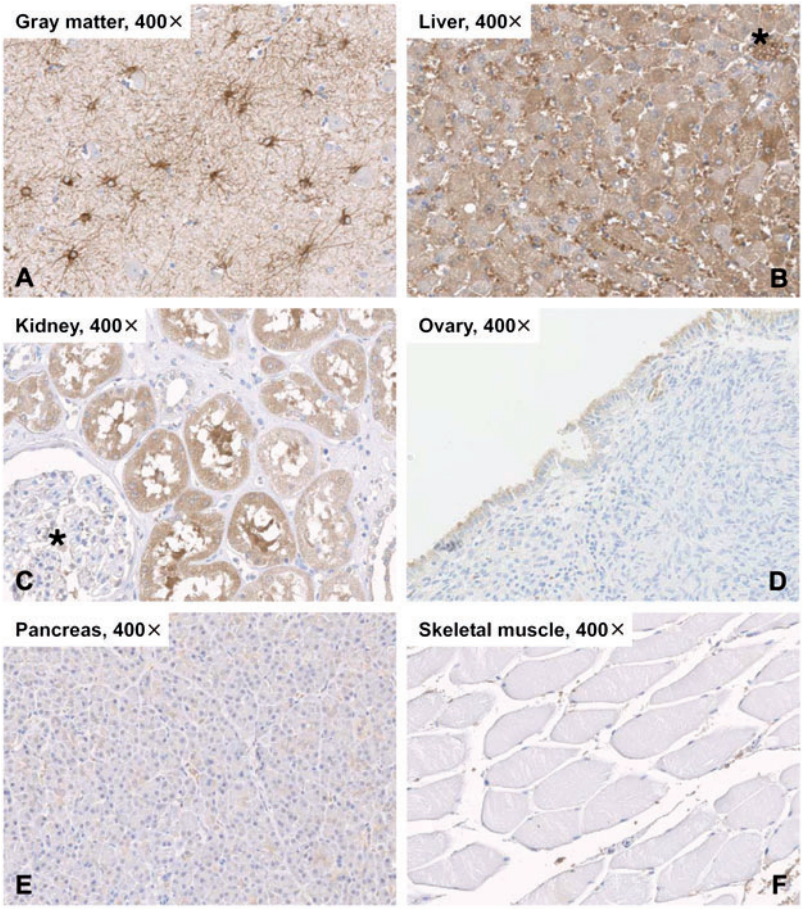

Figure 2 KLK6 immunoexpression pattern in healthy adult human tissues.
Normal tissue sections (A–F) were stained with monospecific pAb 623A using the EnVision system (Dako) (original magnification ×400). (A) In tissue of the central nervous system an intense KLK6 immunostaining was observed in astrocytes, which represent the most frequent glial cell type in gray matter. (B) KLK6 immunoexpression was found in healthy adult liver as illustrated by a distinct, cytoplasmatic staining of hepatocytes. In addition, strong staining of erythrocytes was observed within the hepatic venule (marked with ✱) as well as in the sinusoidal vasculature between the plates of hepatocytes. (C) Moderate KLK6 immunostaining was detected in proximal and distal convoluted tubules of the renal cortex. KLK6 expression was not observed in glomeruli (marked with ✱). Micrograph (D) displays moderate, cytoplasmic KLK6 staining within the surface epithelium of the normal ovary consisting of a single layer of cuboidal to columnar cells. KLK6 was not detected in the underlying stroma harboring cells with round and spindle-shaped morphology, most of which are probably derived from cells of fibroblastic type. (E, F) There was no KLK6 immunoexpression in glandular cells of the exocrine pancreas or in skeletal muscle.

immunoexpression values were marginally, but significantly, related with shorter PFS, whereas there was no significance for OS (association with PFS: HR, 1.68; 95% CI, 1.02–2.76; p=0.042; association with OS: HR, 1.51; 95% CI, 0.95–2.39; p=0.080; Table 2). These findings were confirmed by Kaplan-Meier estimation, the association of KLK6-Tc and KLK6-Sc expression levels with OS and PFS is displayed in the respective survival curves (Figure 4).

Strikingly, in multivariate analysis, KLK6-Sc score values were significantly associated with poor OS, i.e., ovarian cancer patients with high KLK6-Sc immunoexpression in tumor tissue had a significantly, nearly twofold higher risk of death (HR, 1.92; 95% CI, 1.12–3.27; p=0.017) as compared with patients who displayed low KLK6-Sc expression levels (Table 3). Although displaying only a trend in univariate analysis, patients with high KLK6-Sc score values turned out to have a nearly twofold higher risk of disease progression in multivariate analysis (HR 1.80; 95% CI, 1.02–3.19; p=0.042; Table 3). On the contrary, in multivariate analysis, KLK6 immunoexpression in tumor cells (KLK6-Tc) was not significantly related with OS or PFS of ovarian cancer patients (Table 3).

Finally, concerning the clinical parameters, in multivariate Cox analysis, residual tumor mass and FIGO stage remained strong, statistically significant parameters for both shorter OS and PFS. All other clinical and histomorphological markers analyzed lost significance for OS and PFS in ovarian cancer patients in multivariate analysis (Table 3).

Discussion

In the present study, we used monospecific polyclonal antibodies (pAb 623A) that were affinity-purified against a unique KLK6 peptide encompassing amino acids 109 to 119.

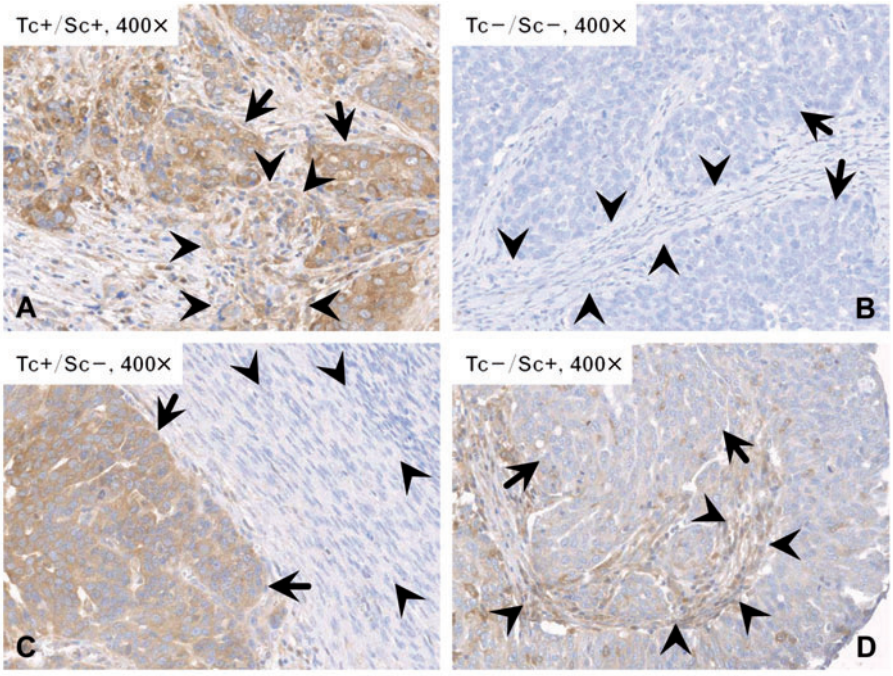

Figure 3 KLK6 immunoexpression in tumor tissue of ovarian cancer specimens.
Tissue sections were stained with monospecific pAb 623A using the EnVision system (Dako) (original magnification ×400). Micrographs (A–D) illustrate representative core punches corresponding to high (+) or low (-) KLK6 immunoexpression in tumor cells (Tc) and stromal cells (Sc), respectively. Arrows indicate staining of tumor cells; stromal cells are marked by arrowheads.

Previous structural analyses show that this linear sequence is exposed on the surface of both the mature form and the pro-form of KLK6 (Bernett et al., 2002; Gomis-Rüth et al., 2002). Consistent with these data, in our study, pAb 623A reacted with both the recombinant mature KLK6 (in one-side ELISA assays; data not shown) and the recombinant pro-form of KLK6 in Western blot analysis (Figure 1A). Importantly, $KLK6_{109–119}$ lacks homology toward respective regions of other KLKs (Goettig et al., 2010). In fact, for all of the recombinant pro-forms from KLK3–5 and KLK7–15, no cross-reaction was observed in Western blot analysis (Figure 1A). Furthermore, pAb 623A strongly reacted with a protein of about 43 kDa in brain tissue extracts, whereas tissue extracts of skeletal muscle, known not to express KLK6 (Shaw and Diamandis, 2007), were negative (Figure 1B). The higher molecular weight of KLK6 (as well as the rather broad signal in Western blot analysis) originating from brain tissue extracts as compared with recombinant, non-glycosylated KLK6 expressed in *Escherichia coli* is attributable to N-glycosylation of KLK6, as reported previously by Kuzmanov et al. (2009).

In previous studies KLK6 expression has already been surveyed in normal human tissues at the mRNA as well as protein level by highly specific PCR and ELISA assays (Harvey et al., 2000; Shaw and Diamandis, 2007). The highest KLK6 expression was reported for the CNS, followed by kidney, breast, ovary, and skin tissue. By comparison, healthy human adult tissues of the liver, lung, heart, and spleen showed low KLK6 levels, whereas in the colon, skeletal muscle, prostate, and pancreas, KLK6 expression was not detected. Using pAb 623A to assess KLK6 expression by immunohistochemistry, we observed a very similar staining pattern to that described by Shaw and Diamandis (2007). In Western blot analysis, KLK6 was detected in white and gray matter as well as in undivided brain tissue encompassing both white and gray matter (Figure 1B), implicating that KLK6 might be expressed by cells that are distributed throughout the entire human brain. However, by immunohistochemistry, we localized KLK6 expression exclusively in the astrocytes (Figure 2A), which represent the most numerous glial cells in gray matter. These findings are in line with comprehensive immunohistochemical studies describing weak immunoreactivity of neural cells, but moderate staining of glial cells using polyclonal and monoclonal antibodies directed to KLK6 (Petraki et al., 2001). In general, glial cells, including the astrocytes, are nonneural highly branched cells providing both mechanical and metabolic support to neurons. Particularly, the astrocytes, which are found not only in gray, but also in white matter, exhibit intimate functional relationships with neurons because they mediate the exchange of metabolites between neurons and the vascular system and are also partly forming the blood-brain barrier. Nevertheless, what seems even more interesting is the fact that astrocytes are known to participate in the repair of CNS tissue after injury or damage by disease. Therefore, KLK6 expression restricted to astrocytes as detected by pAb 623A is supporting previous findings postulating contribution of KLK6 to the process of axon outgrowth following spinal cord injury as well as to the progression of neurodegenerative

Table 1 Association of clinical and histomorphological characteristics with KLK6 immunoexpression in tumor vs. stromal cells in ovarian cancer patients (n=118).

Clinical/histomorphological parameters	Patient numbers	KLK6-Tc low/high	KLK6-Sc[a] low/high
Total	118	84/34	93/24
Age		p=0.291	p=0.791
≤60 years	71	48/23	57/14
>60 years	47	36/11	36/10
FIGO stage		p=0.141	p=0.275
I+II	24	20/4	21/3
III+IV	94	64/30	72/21
Nuclear grade		p=0.966	p=0.028*
G1+G2	42	30/12	38/4
G3	76	54/22	55/20
Residual tumor mass[b]		p=0.113	p=0.276
0 cm	61	47/14	50/10
>0 cm	52	33/19	39/13
Ascitic fluid volume[b]		p=0.423	p=0.512
≤500 ml	74	54/20	59/14
>500 ml	41	27/14	31/10
Lymph nodes involved[b]		p=0.201	p=0.020*
No	43	34/9	38/4
Yes	52	35/17	37/15
Response to CT[b]		p=0.945	p=0.746
No	17	12/5	13/4
Yes	76	53/23	60/15

χ^2-Test (cutoff point: median score values).
[a]No. of cases n=117.
[b]The number of cases does not add up to 118 due to missing clinical data.
*Statistically significant values ($p \leq 0.05$).

diseases (Scarisbrick et al., 2006, 2008; Hebb et al., 2010). Furthermore, involvement of KLK6 in intracellular signaling by targeting protease-activated receptors (PARs) has also been studied. In fact, KLK6 was shown to activate astrocytic receptors PAR1 and PAR2, thus contributing to glial scarring in CNS (Vandell et al., 2008).

We further investigated KLK6 protein expression by immunohistochemistry in tumor tissues of 118 ovarian cancer patients applying pAb 623A. Distinct cytoplasmic immunostaining was detected in both malignant epithelial tumor cells and, with lower frequency, in surrounding stromal cells (Figure 3). We assume these KLK6 expressing stromal cells to be fibroblasts and tissue macrophages due to their distinct morphology in histology. In the white matter of injured spinal cord, in fact, CD68-positive macrophages have been reported to abundantly express KLK6 (Scarisbrick et al., 2006). Strikingly, we observed a statistically significant correlation between stromal cell-associated KLK6 expression (KLK6-Sc) and disease survival: in multivariate analyses, ovarian cancer patients with high KLK6-Sc immunoexpression in their tumor tissue faced both a significantly shorter OS and PFS as compared with patients who displayed low KLK6-Sc expression levels in their tumor tissue (Table 3). In ovarian cancer, elevated KLK6 mRNA and protein levels have indeed repeatedly been observed and already been related to poor disease outcome of the patients (Hoffmann et al., 2002; Luo et al., 2006; Kountourakis et al., 2008; Bayani et al., 2011; Koh et al., 2011). However, to our knowledge, this is the first study demonstrating that stromal cell-associated KLK6 expression significantly affects patients' prognosis. Previous studies concerning KLK4 protein expression in breast cancer have reported up-regulation of KLK4 in the tumor stroma (Mangé et al., 2008), although its clinical significance was not investigated. Additionally, enhanced KLK4 expression has also been identified in the effusions and stroma of invasive epithelial ovarian cancers (Davidson et al., 2005) and was associated predominantly with primary cancers over metastases. However, no association was found between KLK4 stromal expression and survival, in contrast to the data presented here for KLK6.

To date, KLK6 has shown a wide range of functional diversity with respect to carcinogenesis (Bayani and Diamandis, 2011); however, our understanding of its contribution in the reactive stroma to the tumor microenvironment is only beginning to emerge. In a recent study, the expression pattern of KLK6 was investigated in cutaneous malignant melanoma (Krenzer et al., 2011). Interestingly, KLK6 was not detectable in tumor cells, but a strong KLK6 protein expression was found in stromal cells and keratinocytes adjacent to tumor cells and a paracrine function of secreted KLK6 during neoplastic transformation and malignant progression was suggested. In fact, when recombinant KLK6 was added to melanoma cells *in vitro*, both cell migration and cell invasion were induced, accompanied by an activation of the signaling receptor PAR1 (Krenzer et al., 2011). In biochemical *in vitro* studies, KLK6 was shown to cleave prominent components of the tumor stroma, such as fibronectin as well as different types of collagen (Magklara et al., 2003; Borgoño and Diamandis, 2004; Ghosh et al., 2004), which may indeed support tissue remodeling, tumor invasion, and metastasis.

In conclusion, our immunohistochemical study provides evidence that, in ovarian cancer, both tumor and surrounding stromal cells frequently overexpress KLK6. Because, especially, stromal cell-associated KLK6 expression in tumor tissue was found to be significantly related to shortened OS and PFS in ovarian cancer patients, stromal cell-derived KLK6 may considerably contribute to the aggressiveness of ovarian neoplasms.

Materials and methods

Recombinant KLK6

Recombinant KLK6, harboring an N-terminal $(His)_6$-tag followed by an enterokinase cleavage site, was expressed in *E. coli* and purified as described previously (Debela et al., 2006a,b). Expressed (non-glycosylated) protein was purified *via* its histidine-tag by nickel-nitrilotriacetic acid agarose affinity chromatography (Qiagen, Hilden, Germany) under denaturing/slightly reducing conditions. Subsequently, refolding procedures were used, using reduced and oxidized glutathione as redox reagents (Sigma, Deisenhofen, Germany) to promote protein renaturation. In addition to rec-KLK6, recombinant pro-forms of KLK proteases (KLK2 to KLK15) plus an N-terminally located $(His)_6$-tag and a C-terminal Tag100 epitope were produced and purified in a similar manner as described (Seiz et al., 2010).

Table 2 Univariate Cox regression analysis of the association of clinical and histomorphological parameters and KLK6 immunoexpression with disease survival in ovarian cancer patients (n=118).

Factor	No. cases	OS		PFS	
		HR (95% CI)[a]	*p*-Value	HR (95% CI)[a]	*p*-Value
Total number	118				
Age					
≤60 years	71	1		1	
>60 years	47	1.76 (1.14–2.72)	0.011*	1.67 (1.03–2.69)	0.036*
FIGO stage					
I+II	24	1		1	
III+IV	94	6.12 (2.64–14.1)	<0.001*	10.4 (3.25–33.3)	<0.001*
Nuclear grade					
G1+G2	42	1		1	
G3	76	2.02 (1.24–3.28)	0.005*	1.80 (1.06–3.07)	0.030*
Residual tumor mass[b]					
0 mm	61	1		1	
>0 mm	52	5.74 (3.51–9.40)	<0.001*	5.50 (3.24–9.32)	<0.001*
Ascitic fluid volume[b]					
≤500 ml	74	1		1	
>500 ml	41	3.69 (2.35–5.80)	<0.001*	3.29 (1.99–5.43)	<0.001*
KLK6-Tc[c]					
Low	84	1		1	
High	34	1.51 (0.95–2.39)	0.080	1.68 (1.02–2.76)	0.042*
KLK6-Sc[c,d]					
Low	93	1		1	
High	24	1.80 (1.08–2.99)	0.024*	1.68 (0.97–2.92)	0.066

[a]HR (95% CI) of univariate Cox regression analysis.
[b]The number of cases does not add up to 118 due to missing clinical data.
[c]Dichotomized in high and low levels by the median score values.
[d]No. of cases, n=117.
*Statistically significant data ($p \leq 0.05$).

Generation of polyclonal antibodies against rec-KLK6

At the Department of Laboratory Medicine of the Radboud University, Nijmegen Medical Centre (Nijmegen, The Netherlands), rabbits were immunized by injection of purified, refolded human rec-KLK6, carrying the N-terminal $(His)_6$-tag and EK cleavage site, first into the popliteal lymph gland and then subcutaneously following the protocol by McKiernan et al. (2008). After 12 booster vaccinations (i.e., about 5 months after beginning of the immunization), the rabbits were sacrificed, and (citrated) plasma was generated from collected blood and stored at -80°C.

Purification of polyclonal antibody 623A by affinity chromatography

Polyclonal antibodies from animal #623 (pAb 623A) were purified using an affinity column that contained an equal mixture of AffiGel®10 and AffiGel®15 (Bio-Rad, Hercules, CA, USA) with covalently linked peptide $KLK6_{109–119}$, following the strategy previously used to purify monospecific antibodies against recombinant KLK4 (Seiz et al., 2010). The yield of purified, monospecific pAb 623A was 0.24 mg from 4 ml of unpurified plasma used for the purification.

Peptides $KLK6_{109–119}$, GSHHHHHHGS, and HHHGSDDDDK (corresponding to $(His)_6$-tag and the EK cleavage site of rec-KLK6, respectively) were synthesized by the Service Center of the Max-Planck-Institute of Biochemistry, Martinsried, Germany.

Western blot analysis

Proteins were denatured in the presence of 2% (w/v) sodium dodecyl sulfate and 5% (v/v) 2-mercaptoethanol for 5 min at 95°C, followed by 12% SDS-PAGE. Separated proteins were then transferred onto polyvinylidene fluoride (PVDF) membranes (PALL, Dreieich, Germany) using a semidry system. The membranes were blocked with 5% (v/v) skim milk in PBS for 1 h at room temperature and then incubated overnight with pAb 623A directed to KLK6. Thereafter, bound antibodies were detected by horseradish peroxidase-conjugated goat anti-rabbit IgG (Jackson ImmunoResearch Lab, West Grove, PA, USA; dilution: 1:10 000), followed by an enhanced chemiluminescence reaction (Amersham Biosciences, Little Chalfont, UK). To define the relative molecular mass of positive bands, the prestained Protein IV-Marker set (PeqLab, Erlangen, Germany) was used.

Patients and tissues

One hundred eighteen patients afflicted with ovarian cancer stages FIGO I–IV (Fédération Internationale de Gynécologie et d'Obstétrique), treated at the Department of Obstetrics and Gynecology of the Technical University of Munich between 1992 and 1999, were enrolled in this retrospective study. The study was approved by the Ethics Committee of the Klinikum rechts der Isar, Technical University of Munich.

Patients' age at diagnosis ranged from 20 to 85 years (median, 57 years). All patients initially underwent the standard stage-related

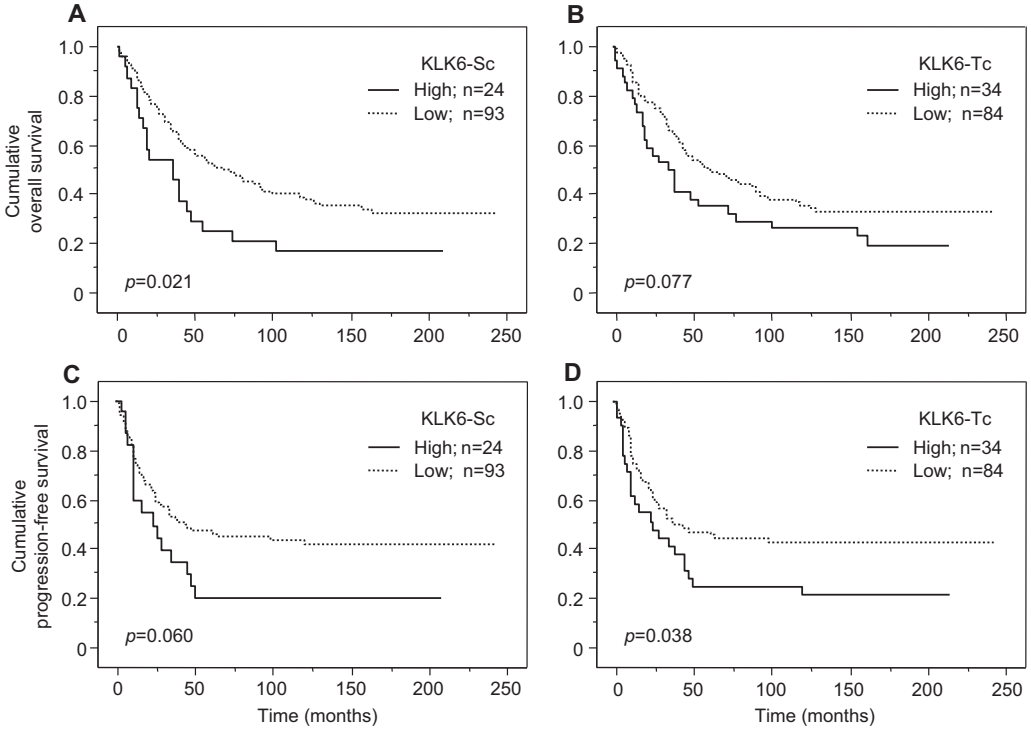

Figure 4 Probability of OS and PFS of ovarian cancer patients with regard to KLK6 immunoexpression.
(A, B) OS and (C, D) PFS probability curves were generated by Kaplan-Meier analysis using log-rank tests to search for differences. Patients were divided into groups with low or high KLK6 immunoexpression in stromal cells (A, C) and tumor cells (B, D) using the median score values (KLK6-Sc, 0 vs. >0; KLK6-Tc, ≤4 vs. >4).

Table 3 Multivariate Cox regression analysis of the association of clinical and histomorphological parameters and KLK6 immunoexpression with disease survival in ovarian cancer patients (n=110).

Factor	No. cases	OS		PFS	
		HR (95% CI)[a]	*p*-Value	HR (95% CI)[a]	*p*-Value
Total number	110				
FIGO stage					
I+II	21	1		1	
III+IV	89	3.13 (1.18–8.26)	0.021*	4.96 (1.47–16.7)	0.010*
Nuclear grade					
G1+G2	38	1		1	
G3	72	1.28 (0.76–2.15)	0.350	0.95 (0.54–1.68)	0.868
Residual tumor mass					
0 mm	60	1		1	
>0 mm	50	3.32 (1.73–6.39)	<0.001*	3.21 (1.64–6.26)	<0.001*
Ascitic fluid volume					
≤500 ml	73	1		1	
>500 ml	37	1.27 (0.71–2.33)	0.406	1.31 (0.70–2.47)	0.392
KLK6-Tc[b]					
Low	77	1		1	
High	33	1.18 (0.73–1.91)	0.507	1.26 (0.75–2.10)	0.387
KLK6-Sc[b,c]					
Low	86	1		1	
High	23	1.92 (1.12–3.27)	0.017*	1.80 (1.02–3.19)	0.042*

[a]HR (95% CI) of multivariate Cox regression analysis. Biological markers were separately added to the base model of clinical parameters: FIGO stage, nuclear grade, residual tumor mass, and ascitic fluid volume.
[b]Dichotomized in high and low levels by the median score values.
[c]No. of cases, n=109.
*Statistically significant data (p=0.05).

primary radical debulking operation, including hysterectomy, bilateral adnectomy, infragastric omentectomy, and pelvic and paraaortic lymphadenectomy if indicated as well as removal of all existing tumor if possible. Sixty-one patients (51.7%) were optimally debulked with complete removal of macroscopically visible tumor manifestations. Surgical specimens were histologically examined at the Institute of Pathology of the Technical University of Munich.

After surgical treatment, 106 (89.8%) patients received adjuvant, platinum-containing chemotherapy as recommended individually for each patient by a multidisciplinary tumor board. Due to unfavorable health conditions, 10 patients received no adjuvant therapy, whereas two women were subjected to nonplatinum regimens for first-line chemotherapy. After this multimodal guideline therapy, 68 (57.6%) patients experienced disease recurrence. Median observation time for all of the patients was 51 months (range, 1–244 months). For those 36 women still alive at time of recent follow-up in March 2011, the median observation time was 173 months (range, 14–244 months). Patient and tumor characteristics are listed in Table 1.

Tissue preparation and microarray construction

Patients' tissue samples were obtained during surgery, inspected by a pathologist from the Institute of Pathology of the Technical University of Munich, and immediately fixed in neutral buffered formalin and embedded in paraffin. Tissue microarrays were constructed using previously established and validated techniques (Wan et al., 1987; Skacel et al., 2002). First, routine hematoxylin and eosin (H&E)-stained sections were prepared for each individual tumor sample. Morphologically representative areas were marked on the original H&E slides by the pathologist. Using these slides for orientation, three cylindrical core biopsies of 1 mm in diameter were carefully lifted from the selected areas of each individual paraffin-embedded tumor tissue (donor block) and precisely mounted into a paraffin block (recipient block) with the help of a manual tissue microarray device (MTA-1, Beecher, WI, USA). According to their predefined coordinates, the core biopsies were positioned into a grid of empty cylindrical holes prepared on the recipient block. Seven tissue microarray blocks were constructed this way. In addition, various tissues from healthy human adults were obtained from the archives of the Institute of Pathology of the Technical University of Munich. Core punches from these routinely processed, formalin-fixed, paraffin-embedded (FFPE) tissue blocks were assembled on a tissue microarray that was used to evaluate the tissue expression pattern of KLK6.

Using a standard routine microtome (Microm HM335E; Thermo Scientific, Germany), 2-µm-thick sections were cut from the tissue microarray blocks and transferred to electrostatically charged glass slides. For subsequent deparaffinization, the slides were finally dried overnight at 35°C.

Immunohistochemistry

Sections of tissue microarrays as well as conventional sections were stained using rabbit pAb 623A. The tissue sections were dewaxed, rehydrated, and treated for antigen retrieval by pressure cooking (4 min, 120°C, 0.1 M citrate buffer, pH 6.0). After several washes with Tris-buffered saline (TBS, pH 7.6), a dual enzyme block containing 0.5% H_2O_2 was applied for 10 min at room temperature to block both endogenous peroxidase and alkaline phosphatase activity. Subsequently, the primary antibody pAb 623A was allowed to react overnight at 4°C. For detection of tissue-bound pAb 623A, a horseradish peroxidase-labeled polymer comprising secondary antibodies with anti-rabbit and anti-mouse specificity (EnVision; Dako, Hamburg, Germany) was applied to the slides for 30 min at room temperature. The peroxidase reaction was developed with 3,3′-diaminobenzidine (DAB^+; Dako) for 7.5 min at room temperature. Finally, counterstaining of sections was performed with Mayer's hematoxylin solution. As a negative control, the primary antibody was omitted and replaced by green antibody diluent (Dako) or by irrelevant antibodies.

Quantification of KLK6 immunostaining on tissue microarrays

For evaluation of KLK6 immunostaining intensity and location, a semiquantitative score (Remmele score) based on staining intensity and percentage of positive cells was applied. For this, staining intensity was classified on a scale of 0–3 (0, no staining; 1, weak staining; 2, moderate staining; 3, strong staining). The percentage of positively stained cells was scored by cell counts after examination of tissue cores on a scale of 0–4 (0, no staining; 1, staining of 1%–10% of cells; 2, 11%–50%; 3, 51%–80%; 4, >80%). The final immunoreactivity score (IRS) was created by multiplication of the intensity score values with the positivity score values, thus obtaining a score between 0 and 12. As for each individual tumor sample, three tissue cores were evaluated, and the mean IRS values of the three readings were used for statistical calculations.

Statistical analysis

The relationship of KLK6 immunoexpression levels (grouped according to their median values) with clinical and histomorphological parameters was determined using the χ^2-test. For survival analyses, both PFS and OS of ovarian cancer patients were used as follow-up end points. The association of KLK6 immunoexpression, as well as of clinical/histomorphological factors with OS and PFS, was analyzed using Cox univariate and multivariate proportional hazards regression models and finally expressed as HR with its 95% confidence interval (95% CI). The multivariate Cox regression model was adjusted for known ovarian cancer-related prognostic factors: FIGO stage, nuclear grade, residual tumor after surgery, and ascitic fluid volume. Survival curves were plotted according to Kaplan-Meier using log-rank tests to recognize differences. All calculations were performed using the StatView 5.0 statistical package (SAS Institute, Cary, NC, USA). *p*-Values ≤0.05 were considered statistically significant.

Acknowledgments

This study was supported in part by grants from the Kommission Klinische Forschung der TU München and from the German Federal Ministry of Education and Research, Leading-Edge Cluster m4. The excellent technical assistance of Sabine Creutzburg and Daniela Hellmann is gratefully acknowledged. We especially thank Karin Mengele and Jürgen Schlegel for helpful discussions and provision of brain protein extracts.

References

Ashby, E.L., Kehoe, P.G., and Love, S. (2010). Kallikrein-related peptidase 6 in Alzheimer's disease and vascular dementia. Brain Res. *1363*, 1–10.

Bayani, J. and Diamandis, E.P. (2011). Review: the physiology and pathobiology of human kallikrein-related peptidase 6 (KLK6). Clin. Chem. Lab. Med. Nov 3 [Epub ahead of print].

Bayani, J., Marrano, P., Graham, C., Zheng, Y., Li, L., Katsaros, D., Lassus, H., Butzow, R., Squire, J.A., and Diamandis, E.P. (2011). Genomic instability and copy-number heterogeneity of chromosome 19q, including the kallikrein locus, in ovarian carcinomas. Mol. Oncol. *5*, 48–60.

Bayés, A., Tsetsenis, T., Ventura, S., Vendrell, J., Aviles, F.X., and Sotiropoulou, G. (2004). Human kallikrein 6 activity is regulated via an autoproteolytic mechanism of activation/inactivation. Biol. Chem. *385*, 517–524.

Beaufort, N., Plaza, K., Utzschneider, D., Schwarz, A., Burkhart, J.M., Creutzburg, S., Debela, M., Schmitt, M., Ries, C., and Magdolen, V. (2010). Interdependence of kallikrein-related peptidases in proteolytic networks. Biol. Chem. *391*, 581–587.

Bernett, M.J., Blaber, S.I., Scarisbrick, I.A., Dhanarajan, P., Thompson, S.M., and Blaber, M. (2002). Crystal structure and biochemical characterization of human kallikrein 6 reveals that a trypsin-like kallikrein is expressed in the central nervous system. J. Biol. Chem. *277*, 24562–24570.

Borgoño, C.A. and Diamandis, E.P. (2004). The emerging roles of human tissue kallikreins in cancer. Nat. Rev. Cancer *4*, 876–890.

Christophi, G.P., Isackson, P.J., Blaber, S., Blaber, M., Rodriguez, M., and Scarisbrick, I.A. (2004). Distinct promoters regulate tissue-specific and differential expression of kallikrein 6 in CNS demyelinating disease. J. Neurochem. *91*, 1439–1449.

Davidson, B., Xi, Z., Klokk, T.I., Tropé, C.G., Dørum, A., Scheistrøen, M., and Saatcioglu, F. (2005). Kallikrein 4 expression is up-regulated in epithelial ovarian carcinoma cells in effusions. Am. J. Clin. Pathol. *123*, 360–368.

Debela, M., Magdolen, V., Grimminger, V., Sommerhoff, C., Messerschmidt, A., Huber, R., Friedrich, R., Bode, W., and Goettig, P. (2006a). Crystal structures of human tissue kallikrein 4: activity modulation by a specific zinc binding site. J. Mol. Biol. *362*, 1094–1107.

Debela, M., Magdolen, V., Schechter, N., Valachova, M., Lottspeich, F., Craik, C.S., Choe, Y., Bode, W., and Goettig, P. (2006b). Specificity profiling of seven human tissue kallikreins reveals individual subsite preferences. J. Biol. Chem. *281*, 25678–25688.

Debela, M., Beaufort, N., Magdolen, V., Schechter, N.M., Craik, C.S., Schmitt, M., Bode, W., and Goettig, P. (2008). Structures and specificity of the human kallikrein-related peptidases KLK 4, 5, 6, and 7. Biol. Chem. *389*, 623–632.

Diamandis, E.P., Yousef, G.M., Luo, L.-Y., Magklara, A., and Obiezu, C.V. (2000). The new human kallikrein gene family: implications in carcinogenesis. Trends Endocrinol. Metab. *11*, 54–60.

Diamandis, E.P., Scorilas, A., Fracchioli, S., Van Gramberen, M., De Bruijn, H., Henrik, A., Soosaipillai, A., Grass, L., Yousef, G.M., Stenman, U.H., et al. (2003). Human kallikrein 6 (hK6): a new potential serum biomarker for diagnosis and prognosis of ovarian carcinoma. J. Clin. Oncol. *21*, 1035–1043.

Dorn, J., Schmitt, M., Kates, R., Schmalfeldt, B., Kiechle, M., Scorilas, A., Diamandis, E.P., and Harbeck, N. (2007). Primary tumor levels of human tissue kallikreins affect surgical success and survival in ovarian cancer patients. Clin. Cancer Res. *13*, 1742–1748.

Emami, N. and Diamandis, E.P. (2008). Utility of kallikrein-related peptidases (KLKs) as cancer biomarkers. Clin. Chem. *54*, 1600–1607.

Ghosh, M.C., Grass, L., Soosaipillai, A., Sotiropoulou, G., and Diamandis, E.P. (2004). Human kallikrein 6 degrades extracellular matrix proteins and may enhance the metastatic potential of tumour cells. Tumour Biol. *25*, 193–199.

Goettig, P., Magdolen, V., and Brandstetter, H. (2010). Natural and synthetic inhibitors of kallikrein-related peptidases (KLKs). Biochimie *92*, 1546–1567.

Gomis-Rüth, F.X., Bayés, A., Sotiropoulou, G., Pampalakis, G., Tsetsenis, T., Villegas, V., Avilés, F.X., and Coll, M. (2002). The structure of human prokallikrein 6 reveals a novel activation mechanism for the kallikrein family. J. Biol. Chem. *277*, 27273–27281.

Harvey, T.J., Hooper, J.D., Myers, S.A., Stephenson, S.A., Ashworth, L.K., and Clements, J.A. (2000). Tissue-specific expression patterns and fine mapping of the human kallikrein (KLK) locus on proximal 19q13.4. J. Biol. Chem. *275*, 37397–37406.

Hebb, A.L., Bhan, V., Wishart, A.D., Moore, C.S., and Robertson, G.S. (2010). Human kallikrein 6 cerebrospinal levels are elevated in multiple sclerosis. Curr. Drug Discov. Technol. *7*, 137–140.

Hoffman, B.R., Katsaros, D., Scorilas, A., Diamandis, P., Fracchioli, S., Rigault de la Longrais, I.A., Colgan, T., Puopolo, M., Giardina, G., et al. (2002). Immunofluorometric quantitation and histochemical localisation of kallikrein 6 protein in ovarian cancer tissue: a new independent unfavourable prognostic biomarker. Br. J. Cancer *87*, 763–771.

Iwata, A., Maruyama, M., Akagi, T., Hashikawa, T., Kanazawa, I., Tsuji, S., and Nukina, N. (2003). Alpha-synuclein degradation by serine protease neurosin: implication for pathogenesis of synucleinopathies. Hum. Mol. Genet. *12*, 2625–2635.

Koh, S.C., Razvi, K., Chan, Y.H., Narasimhan, K., Ilancheran, A., Low, J.J., and Choolani, M. [Ovarian Cancer Research Consortium of SE Asia] (2011). The association with age, human tissue kallikreins 6 and 10 and hemostatic markers for survival outcome from epithelial ovarian cancer. Arch. Gynecol. Obstet. *284*, 183–190.

Kountourakis, P., Psyrri, A., Scorilas, A., Camp, R., Markakis, S., Kowalski, D., Diamandis, E.P., and Dimopoulos, M.A. (2008). Prognostic value of kallikrein-related peptidase 6 protein expression levels in advanced ovarian cancer evaluated by automated quantitative analysis (AQUA). Cancer Sci. *99*, 2224–2229.

Krenzer, S., Peterziel, H., Mauch, C., Blaber, S.I., Blaber, M., Angel, P., and Hess, J. (2011). Expression and function of the kallikrein-related peptidase 6 in the human melanoma microenvironment. J. Investig. Dermatol. *131*, 2281–2288.

Kuzmanov, U., Jiang, N., Smith, C.R., Soosaipillai, A., and Diamandis, E.P. (2009). Differential N-glycosylation of kallikrein 6 derived from ovarian cancer cells or the central nervous system. Mol. Cell. Proteomics *8*, 791–798.

Lundwall, A. and Brattsand, M. (2008). Kallikrein-related peptidases. Cell. Mol. Life Sci. *65*, 2019–2038.

Luo, L.-Y. and Jiang, W. (2006). Inhibition profiles of human tissue kallikreins by serine protease inhibitors. Biol. Chem. *387*, 813–816.

Luo, L.-Y., Soosaipillai, A., Grass, L., and Diamandis, E.P. (2006). Characterization of human kallikreins 6 and 10 in ascites fluid from ovarian cancer patients. Tumour Biol. *27*, 227–234.

Magklara, A., Mellati, A.A., Wasney, G.A., Little, S.P., Sotiropoulou, G., Becker, G.W., and Diamandis, E.P. (2003). Characterization of the enzymatic activity of human kallikrein 6: autoactivation, substrate specificity, and regulation by inhibitors. Biochem. Biophys. Res. Commun. *307*, 948–955.

Mangé, A., Desmetz, C., Berthes, M.L., Maudelonde, T., and Solassol, J. (2008). Specific increase of human kallikrein 4 mRNA and protein levels in breast cancer stromal cells. Biochem. Biophys. Res. Commun. *375*, 107–112.

McKiernan, E., O'Brien, K., Grebenchtchikov, N., Geurts-Moespot, A., Sieuwerts, A.M., Martens, J.W., Magdolen, V., Evoy, D.,

McDermott, E., Crown, J., et al. (2008). Protein kinase Cdelta expression in breast cancer as measured by real-time PCR, western blotting and ELISA. Br. J. Cancer *99*, 1644–1650.

Oikonomopoulou, K., Li, L., Zheng, Y., Simon, I., Wolfert, R.L., Valik, D., Nekulova, M., Simickova, M., Frgala, T., and Diamandis, E.P. (2008). Prediction of ovarian cancer prognosis and response to chemotherapy by a serum-based multiparametric biomarker panel. Br. J. Cancer *99*, 1103–1113.

Pampalakis, G. and Sotiropoulou, G. (2007). Tissue kallikrein proteolytic cascade pathways in normal physiology and cancer. Biochim. Biophys. Acta *1776*, 22–31.

Pampalakis, G., Diamandis, E.P., and Sotiropoulou, G. (2006). The epigenetic basis for the aberrant expression of kallikreins in human cancers. Biol. Chem. *387*, 795–799.

Petraki, C.D., Karavana, V.N., Skoufogiannis, P.T., Little, S.P., Howarth, D.J., Yousef, G.M., and Diamandis, E.P. (2001). The spectrum of human kallikrein 6 (zyme/protease M/neurosin) expression in human tissues as assessed by immunohistochemistry. J. Histochem. Cytochem. *49*, 1431–1441.

Petraki, C.D., Papanastasiou, P.A., Karavana, V.N., and Diamandis, E.P. (2006). Cellular distribution of human tissue kallikreins: immunohistochemical localization. Biol. Chem. *387*, 653–663.

Prezas, P., Arlt, M.J., Viktorov, P., Soosaipillai, A., Holzscheiter, L., Schmitt, M., Talieri, M., Diamandis, E.P., Krüger, A., and Magdolen, V. (2006). Overexpression of the human tissue kallikrein genes KLK4, 5, 6, and 7 increases the malignant phenotype of ovarian cancer cells. Biol. Chem. *387*, 807–811.

Rosen, D.G., Wang, L., Atkinson, J.N., Yu, Y., Lu, K.H., Diamandis, E.P., Hellstrom, I., Mok, S.C., Liu, J., and Bast, R.C. Jr. (2005). Potential markers that complement expression of CA125 in epithelial ovarian cancer. Gynecol. Oncol. *99*, 267–277.

Scarisbrick, I.A., Sabharwal, P., Cruz, H., Larsen, N., Vandell, A.G., Blaber, S.I., Ameenuddin, S., Papke, L.M., Fehlings, M.G., Reeves, R.K., et al. (2006). Dynamic role of kallikrein 6 in traumatic spinal cord injury. Eur. J. Neurosci. *24*, 1457–1469.

Scarisbrick, I.A., Linbo, R., Vandell, A.G., Keegan, M., Blaber, S.I., Blaber, M., Sneve, D., Lucchinetti, C.F., Rodriguez, M., and Diamandis, E.P. (2008). Kallikreins are associated with secondary progressive multiple sclerosis and promote neurodegeneration. Biol. Chem. *389*, 739–745.

Seiz, L., Kotzsch, M., Grebenchtchikov, N.I., Geurts-Moespot, A.J., Fuessel, S., Goettig, P., Gkazepis, A., Wirth, M.P., Schmitt, M., Lossnitzer, A., et al. (2010). Polyclonal antibodies against kallikrein-related peptidase 4 (KLK4): immunohistochemical assessment of KLK4 expression in healthy tissues and prostate cancer. Biol. Chem. *391*, 391–401.

Shan, S.J., Scorilas, A., Katsaros, D., and Diamandis, E.P. (2007). Transcriptional upregulation of human tissue kallikrein 6 in ovarian cancer: clinical and mechanistic aspects. Br. J. Cancer *96*, 362–372.

Shaw, J.L. and Diamandis, E.P. (2007). Distribution of 15 human kallikreins in tissues and biological fluids. Clin. Chem. *53*, 1423–1432.

Sidiropoulos, M., Pampalakis, G., Sotiropoulou, G., Katsaros, D., and Diamandis, E.P. (2005). Down-regulation of human kallikrein 10 (KLK10/NES1) by CpG island hypermethylation in breast, ovarian and prostate cancers. Tumour Biol. *26*, 324–336.

Skacel, M., Skilton, B., Pettay, J.D., and Tubbs, R.R. (2002). Tissue microarrays: a powerful tool for high-throughput analysis of clinical specimens: a review of the method with validation data. Appl. Immunohistochem. Mol. Morphol. *10*, 1–6.

Sotiropoulou, G., Pampalakis, G., and Diamandis, E.P. (2009). Functional roles of human kallikrein-related peptidases. J. Biol. Chem. *284*, 32989–32994.

Vandell, A.G., Larson, N., Laxmikanthan, G., Panos, M., Blaber, S.I., Blaber, M., and Scarisbrick, I.A. (2008). Protease-activated receptor dependent and independent signaling by kallikreins 1 and 6 in CNS neuron and astroglial cell lines. J. Neurochem. *107*, 855–870.

Wan, W.H., Fortuna, M.B., and Furmanski, P. (1987). A rapid and efficient method for testing immunohistochemical reactivity of monoclonal antibodies against multiple tissue samples simultaneously. J. Immunol. Methods *103*, 121–129.

White, N.M., Mathews, M., Yousef, G.M., Prizada, A., Fontaine, D., Ghatage, P., Popadiuk, C., Dawson, L., and Doré, J.J. (2009a). Human kallikrein related peptidases 6 and 13 in combination with CA125 is a more sensitive test for ovarian cancer than CA125 alone. Cancer Biomark. *5*, 279–287.

White, N.M., Mathews, M., Yousef, G.M., Prizada, A., Popadiuk, C., and Doré, J.J. (2009b). KLK6 and KLK13 predict tumor recurrence in epithelial ovarian carcinoma. Br. J. Cancer *101*, 1107–1113.

White, N.M., Bui, A., Mejia-Guerrero, S., Chao, J., Soosaipillai, A., Youssef, Y., Mankaruos, M., Honey, R.J., Stewart, R., Pace, K.T., et al. (2010). Dysregulation of kallikrein-related peptidases in renal cell carcinoma: potential targets of miRNAs. Biol. Chem. *391*, 411–423.

Yoon, H., Laxmikanthan, G., Lee, J., Blaber, S.I., Rodriguez, A., Kogot, J.M., Scarisbrick, I.A., and Blaber, M. (2007). Activation profiles and regulatory cascades of the human kallikrein-related peptidases. J. Biol. Chem. *282*, 31852–31864.

Yoon, H., Blaber, S.I., Evans, D.M., Trim, J., Juliano, M.A., Scarisbrick, I.A., and Blaber, M. (2008). Activation profiles of human kallikrein-related peptidases by proteases of the thrombostasis axis. Protein Sci. *17*, 1998–2007.

Yousef, G.M. and Diamandis, E.P. (2001). The new human tissue kallikrein gene family: structure, function, and association to disease. Endocr. Rev. *22*, 184–204.

Yousef, G.M., Kishi, T., and Diamandis, E.P. (2003). Role of kallikrein enzymes in the central nervous system. Clin. Chim. Acta *329*, 1–8.

Received November 15, 2011; accepted January 6, 2012